ISSN (Print) 1226-1750
ISSN (Online) 2233-6656
**Journal of Magnetics** 19(1), 64-67 (2014) http://dx.doi.org/10.4283/JMAG.2014.19.1.064

# Structural and Magnetic Properties of $Ni_{0.6}Zn_{0.4}Fe_2O_4$ Ferrite Prepared by Solid State Reaction and Sol-gel

**Yoon Mi Kwon, Min-Young Lee, Millaty Mustaqima, Chunli Liu, and Bo Wha Lee***

*Department of Physics and Oxide Research Center, Hankuk University of Foreign Studies, YongIn, Gyeonggi 449-791, Korea*

(Received 10 January 2014, Received in final form 11 February 2014, Accepted 11 February 2014)

**$Ni_{0.6}Zn_{0.4}Fe_2O_4$ prepared using solid state reaction and sol-gel methods were compared for their structural and magnetic properties. Due to the much higher annealing temperature used in solid state reaction, the crystalline size was much larger than that of the nanoparticles prepared by sol-gel. The saturation magnetization of sol-gel nanoparticles was higher, and the coercivity was about 2 times larger, compared to the solid state reaction sample. By analyzing the integration intensity of x-ray diffraction peaks (220) and (222), we proposed that the difference in the saturation magnetization might be due to the inversion of cation distribution caused by the different preparation techniques used.**

**Keywords :** NiZn ferrite, nanoparticles, magnetization, coercivity, cation distribution

## 1. Introduction

Spinel ferrites are useful oxide magnetic materials that are favorably used in low and high frequency applications and recording media, due to their versatility in composition, low cost, and high electromagnetic performance [1]. Recently, ferrite materials have shown promising applications in biomedical systems [2, 3], multi-layer chip inductors, electromagnetic interference suppression, and gas sensing [4, 5], which have promoted intensive research interest on nanostructured ferrite materials. The nanosized ferrite particles are able to exhibit unusual magnetic properties, as compared to the bulk materials. These include superparamagnetism, increased Curie temperature, and metastable cation distribution.

The common preparation technique for ferrites is the solid state reaction method, involving high sintering temperature. On the other hand, chemical-based approaches have been widely adopted, in order to prepare ferrite materials at relatively low temperature. To name a few, ferrite nanoparticles have been reported to form easily through the co-precipitation [6, 7], hydrothermal [8], and sol-gel [9, 10] techniques.

In this work, we prepared $Ni_{0.6}Zn_{0.4}Fe_2O_4$ through the solid state reaction and the sol-gel method, then compared their structural and magnetic properties. $NiFe_2O_4$ is an inverse spinel ferrite, in which the tetrahedral (A) sites are occupied by $Fe^{3+}$ ions, and the octahedral (B) sites by $Fe^{3+}$ and $Ni^{2+}$ ions. When doped with Zn, the $Zn^{2+}$ ions prefer to occupy the tetrahedral sites, which results in more trivalent $Fe^{3+}$ cations occupying the octahedral sites. The magnetic moment usually achieves its highest value with Zn composition ~40%. We chose this composition for investigation in this work.

## 2. Experimental Details

The preparation of the NiZn ferrite nanoparticles was carried out by either solid state reaction or sol-gel. For solid state reaction, NiO (99.99%, SIGMA Aldrich), ZnO (99.99%, Alfa Aesar), and $Fe_2O_3$ (99.99%, Alfa Aesar) powders, with a mole ratio of 0.6:0.4:1, were used as the starting materials. The raw materials were mixed, ground, and calcinated at 900ºC. The powder was ground again before being pressed into pellets. The pellet was sintered at 1250ºC in air and cooled to room temperature. For sol-gel preparation, Nickel nitrate [$Ni(NO_3)_2{\cdot}6H_2O$], Zinc nitrate [$Zn(NO_3)_2{\cdot}6H_2O$], and iron nitrate [$Fe(NO_3)_3{\cdot}9H_2O$] were first separately dissolved in 2-methoxyethanol, then the three kinds of metal nitrate solutions were mixed with molar ratio of Ni : Zn : Fe = 0.6 : 0.4 : 2. The total molar concentration of metals was adjusted to be 0.3 M. The


*Corresponding author: Tel: +82-31-330-4362
Fax: +82-31-330-4566, e-mail: bwlee@hufs.ac.kr

mixed solution was stirred at room temperature for 3 h, then heated at 90°C to evaporate all the liquids to form a dried gel. The heating temperature was then increased to burn the precursor gel in a self-propagating combustion manner to remove all organic gradients. Finally, the obtained powder was annealed at 600°C for 1 h in air for crystallization. Hereafter, we will identify the samples as NZ-solid and NZ-sol-gel, depending on their preparation methods.

The crystallinity of the obtained samples was characterized by x-ray diffraction (XRD). The surface morphology and microstructure of the nanoparticles were observed by using scanning electron microscopy (SEM) and transmission electron microscopy (TEM), respectively. For TEM observations, the nanoparticles were first dispersed in acetone, and one drop of the dispersed solution was put on the TEM grid. The magnetic properties of the nanoparticles were measured by Lakeshore 7400 vibrating sample magnetometer (VSM) in the range of 0-1 Tesla.

## 3. Results and Discussion

The ferrite samples prepared with both techniques were confirmed to be single phase with spinel structure, as shown in Fig. 1(a). Overall, the crystallinity of the two types of samples was similar, implying that the sol-gel approach is also a suitable choice to prepare ferrite materials with good crystallinity at low temperature. In Fig. 1(b), the magnified view shows that the position of the dominant diffraction (311) is at 35.46° for NZ-solid, and 35.34° for NZ-sol-gel, indicating the difference in their lattice constants. The average lattice constants of each sample were calculated from the peak positions of (311) and (440), which turned out to be 8.388 Å for NZ-solid, and 8.415 Å for NZ-sol-gel. Therefore, the lattice constant of the samples prepared with solid state reaction showed slightly smaller lattice constant, as compared to that of the ferrites prepared through sol-gel.

The full width at half maximum (FWHM) reflects the crystalline size of the nanoparticles. Fig. 1(b) shows that the FWHM of the (311) diffraction is 0.19° for the NZ-solid, and 0.24° for the NZ-sol-gel nanoparticles. The average crystallite sizes of the nanoparticles were then estimated, using the Scherrer equation [11] $D = 0.9\ \lambda/(\beta\cos\theta)$, where $\lambda$ is the x-ray wavelength (1.5406 Å), and $\beta$ is the broadening of the peak at angle $\theta$, which can be estimated from the FWHM. For the NZ-solid nanoparticles, the crystalline size was estimated to be around ~52 nm; whereas the NZ-sol-gel nanoparticles were around 40 nm. Due to the much higher annealing temperature used in the solid state reaction, it is reasonable to obtain larger

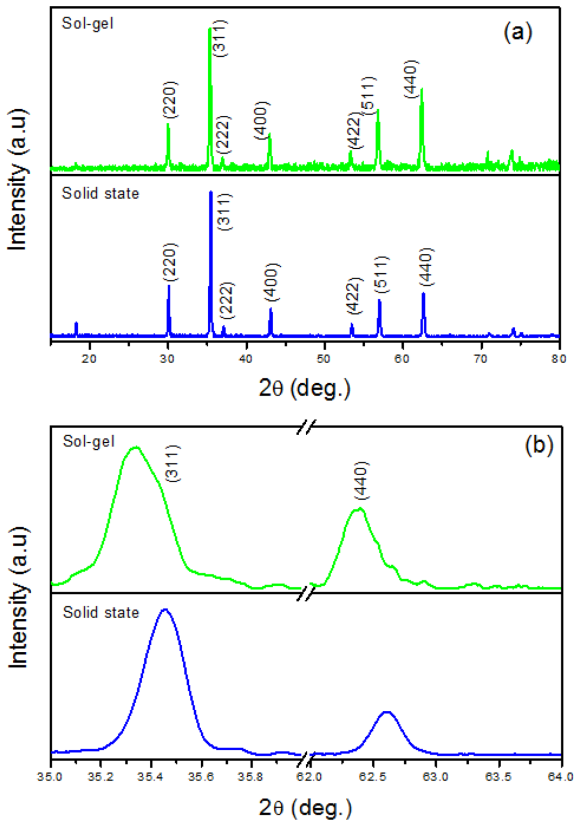


**Fig. 1.** (Color online) (a) XRD spectra of NZ-solid and NZ-sol-gel; and (b) magnified view of (311) and (440) peaks.

crystalline than those prepared by the sol-gel technique.

The morphology and particle size were further characterized through SEM and TEM observations. Fig. 2 shows the SEM images taken from both types of samples. With the magnification of 100 k, the flat surface of the NZ-solid sample in Fig. 2(a) implies that ferrite prepared with solid state reaction actually has quite large grains. In Fig. 2(b), the grains with size around 100 nm or less are clearly seen. Although the estimated crystalline size from the XRD spectra for these two samples were not quite different, the SEM observation gave more direct evidence, showing that the solid state reaction technique produced much larger sized crystalline due to the high sintering temperature used. For NZ-sol-gel, the larger size observed from SEM may be due to the amorphous materials that exist together with the crystals.

The microstructural properties were characterized by TEM. Figs. 3(a) and (b) show an image of the NZ-solid sample and a high resolution image of its lattice; and Figs. 3(c) and (d) are the corresponding images of the NZ-sol-gel sample. The particle size of NZ-sol-gel observed through TEM was quite close to that from SEM, which was around 50 to 100 nm. On the other hand, the particle

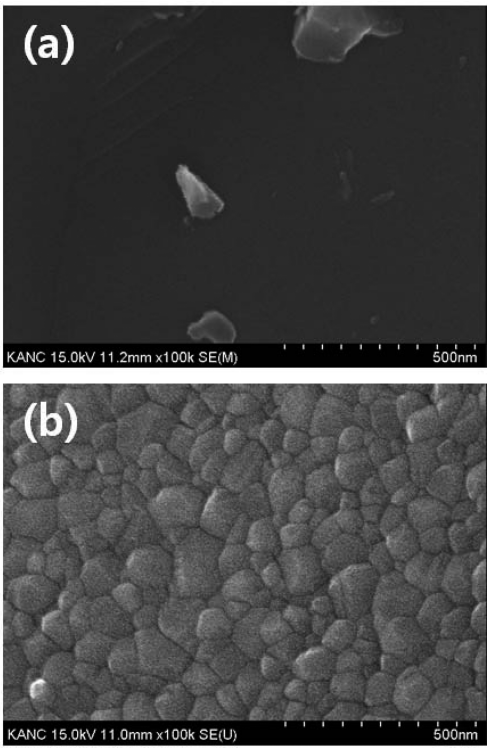


**Fig. 2.** SEM images of (a) NZ-solid, and (b) NZ-sol-gel.

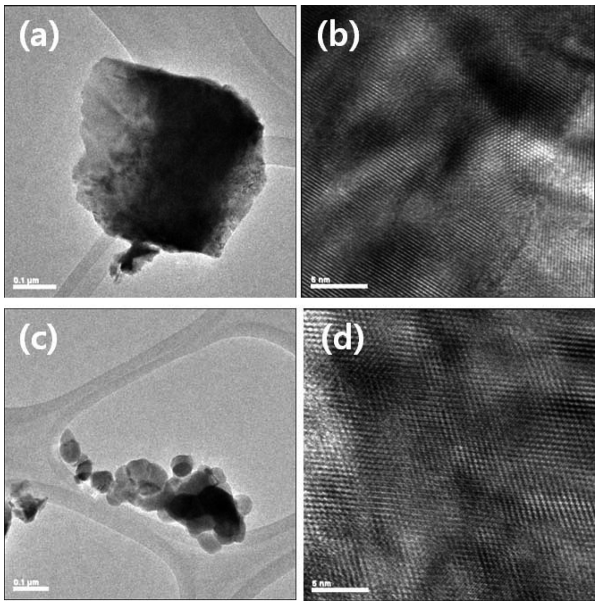


**Fig. 3.** (a) TEM image, and (b) high resolution of lattice image, of the NZ-solid sample. (c) TEM image, and (d) high resolution of lattice image, of the NZ-sol-gel sample.

size was quite big for NZ-solid, showing a size of at least 400 nm in the TEM image. The SEM and TEM observations suggested that the NZ-solid and NZ-sol-gel samples can be considered as bulk materials and nanoparticles,

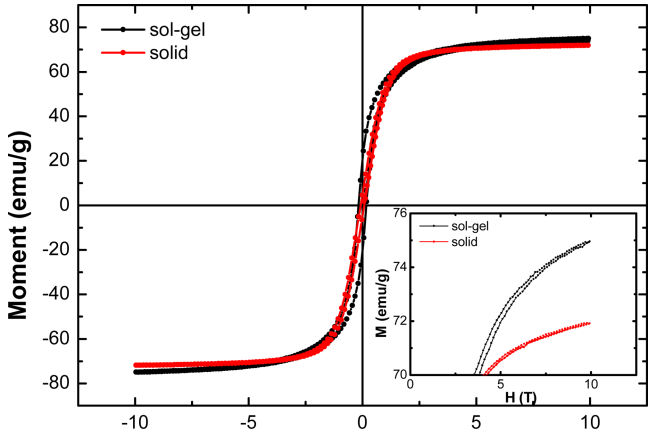


**Fig. 4.** (Color online) Room temperature *M-H* curves of the NZ-solid and NZ-sol-gel samples.

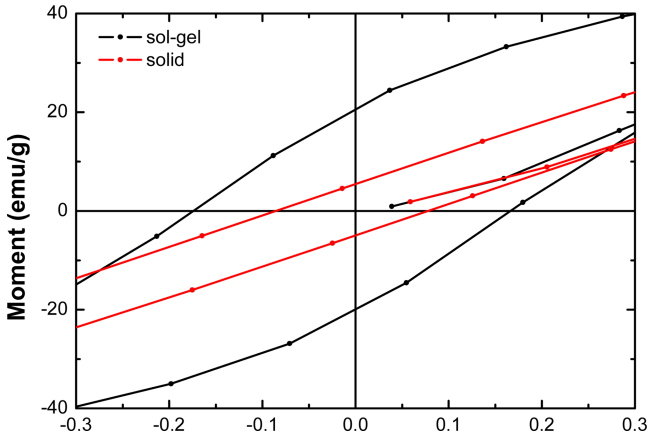


**Fig. 5.** (Color online) The enlarged *M-H* curves near $H$=0, showing the difference between the coercivities.

respectively.

The magnetic properties were studied using VSM at room temperature in the field range of 0-1 Tesla. Although clear hysteresis was observed from both types of samples, the saturation magnetizations ($M_s$) and coercivities ($H_c$) were different. The value of $M_s$ observed from NZ-sol-gel nanoparticles was about 75 emu/g; whereas that of the NZ-solid was about 72 emu/g. The saturation magnetization of $Ni_{0.6}Zn_{0.4}Fe_2O_4$ reported in the literature was of a large range of values, from 30 to the highest value of around 70 emu/g [12-14]. The large diversity of the reported $M_s$ values was due to the preparation techniques and conditions employed by different research groups. The high saturation magnetization observed from both types of samples in our experiment implied their good crystalline quality.

In addition to the saturation magnetization, the coercivity of the NZ-sol-gel nanoparticles was about 173 T as compared to 84 T of the NZ-solid samples. The coercivity

**Table 1.** Measured and calculated parameters for the NZ-solid and NZ-sol-gel.

| Sample/ Parameter | *D* (nm) | Lattice constant (Å) | $M_s$ (emu/g) | $H_c$ (Tesla) | I(220)/ I(222) |
|---|---|---|---|---|---|
| NZ-solid | 52 | 8.388 | 72 | 84 | 4.44 |
| NZ-solgel | 40 | 8.415 | 75 | 173 | 9.95 |

measures the resistance of a ferromagnetic material to a reversed magnetic field, and usually decreases with improved crystallinity due to the existence of less grain boundaries [15]. The increase of $H_c$ can be thought to be due to the increasing grain boundary existed as defects during the magnetization process. Therefore, the much smaller coercivity of NZ-solid indicated a better crystallinity than NZ-sol-gel. Additionally, since the magnetization of ferrite materials is mainly determined by the interactions between $Fe^{3+}$ on the tetrahedral sites and $Fe^{3+}$ on the octahedral sites, NZ-solid should possess higher magnetization as compared to NZ-sol-gel [16]. However, our observation revealed a different result as shown in Fig. 4.

To explain the higher $M_s$ value observed in NZ-sol-gel, factors other than crystallinity should be considered. During the preparation of the nanoparticles, it is possible to have different cation distributions in the lattice other than the theoretical situation due to the experimental conditions used [14, 17]. The variation in the cation distribution can certainly cause the difference in saturation magnetization. To get information of the cation distribution, the integrated peak intensities of the (220) and (222) diffractions in the XRD spectra [14] were calculated, and are listed in Table 1 together with other parameters for the two types of samples. It is seen that the ratio of I(220)/I(222) is higher for NZ-sol-gel. Since the integrated intensity of (220) and (222) reflections depend exclusively on the cations occupying the tetrahedral sites and the octahedral sites, respectively, a smaller value of I(220)/I(222) means a reduction in the concentration of cations that fill the tetrahedral sites, which instead migrate into the octahedral sites. Rao *et al*. reported similar dependence of the saturation magnetization of ferrite nanoparticles with the value of I(220)/I(222) [14]; therefore, the lower $M_s$ observed in NZ-solid, despite its better crystallinity, could be caused by the inversion of cation distribution.

## 4. Conclusions

$Ni_{0.6}Zn_{0.4}Fe_2O_4$ samples were prepared using solid state reaction and sol-gel methods, and their structural and magnetic properties were compared. XRD spectra showed that the sol-gel sample has a little bit larger lattice constant than that of the solid state sample. SEM and TEM both indicated that the solid state reaction technique produced much larger crystalline grains. The NZ-sol-gel showed coercivity of about 2 times that of the NZ-solid, due to the higher density of grain boundaries. Despite the larger grain size, the saturation magnetization of NZ-solid was a little bit lower than that of the NZ-sol-gel, which was explained by considering the inversion of cation distribution suggested by I(220)/I(222).

## Acknowledgement

Bo Wha Lee was supported by the Hankuk University of Foreign Studies Research Fund of 2013.

## References

[1] U. Ozgur, Y. Alivov, and H. Morkoc, J. Mater. Sci.: Mater. Electron. **20**, 789 (2009).
[2] A. Tomitaka, M. Jeun, S. Bae, and Y. Takemura, J. Magnetics **16**, 164 (2011).
[3] I. Sharifi, H. Shokrollahi, and S. Amiri, J. Magn. Magn. Mater. **324**, 903 (2012).
[4] L. Li, L. Peng, Y. Li, and X. Zhu, J. Magn. Magn. Mater. **324**, 60 (2012).
[5] Q. Li, Y. Wang, and C. Chang, J. Alloys. Compd. **505**, 523 (2010).
[6] J. Li, Z. B. Huang, D. W. Wu, G. F. Yin, X. M. Liao, J. W. Gu, and D. Han, J. Phys. Chem. C **114**, 1586 (2010).
[7] S. Ayyappan, S. P. Raja, C. Venkateswaran, J. Philip, and B. Raj, Appl. Phys. Lett. **96**, 143106 (2010).
[8] A. Dias, R. L. Moreira, N. D. S. Mohallem, and A. C. Persiano, J. Magn. Magn. Mater. **172**, L9 (1997).
[9] J. Azadmanjiri, Mater. Chem. Phys. **109**, 109 (2008).
[10] G. Li, X. Zhu, W. Zong, Z. Yang, J. Dai, and Y. Sun, J. Am. Ceram. Soc. **94**, 2872 (2011).
[11] B. D. Cullity, Elements of X-ray Diffraction, 2nd ed. Addison-Wesley, Reading (1978).
[12] S. Verma, P. A. Joy, and S. Kurian, J. Alloys. Compd. **509**, 8999 (2011).
[13] T. J. Shinde, A. B. Gadkari, and P. N. Vasambekar, J. Magn. Magn. Mater. **333**, 152 (2013).
[14] B. Parvatheeswara Rao, G. S. Rao, A. M. Kumar, K. H. Rao, Y. L. Murthy, S. M. Hong, C.-O. Kim, and C. G. Kim, J. Appl. Phys. **101**, 123902 (2007).
[15] K. Sun, Z. Lan, Z. Yu, and X. Nie, Current Appl. Phys. **11**, 472 (2011).
[16] K. P. Chae, W. O. Choi, J.-G. Lee, B.-S. Kang, and S. H. Choi, J. Magnetics **18**, 21 (2013).
[17] E. J. Choi, Y. Ahn, and E. J. Hahn, J. Korean Phys. Soc. **53**, 2090 (2008).